ESSENTIALS OF MULTIANGLE DATA-PROCESSING METHODOLOGY FOR SMOKE POLLUTED ATMOSPHERES*

V. A. KOVALEV, A. PETKOV, C. WOLD, S. URBANSKI, W. M. HAO

U.S. Forest Service, RMRS, Fire Sciences Laboratory,
5775 Highway 10 West, Missoula, Montana, 59808, USA, E-mail: vkovalev@fs.fed.us Email: apetkov@fs.fed.us; E-mail: cewold@fs.fed.us; E-mail: surbanski@fs.fed.us; E-mail: whao@fs.fed.us

Received November 4, 2009

Essentials for investigating smoke plume characteristics with scanning lidar are discussed. Particularly, we outline basic principles for determining dynamics, heights, and optical properties of smoke plumes and layers in wildfire-polluted atmospheres. Both simulated and experimental data obtained in vicinities of wildfires with a two-wavelength scanning lidar are considered.

Key words: Scanning lidar, smoke-polluted atmosphere, measurement methodology.

1. INTRODUCTION

Recent decades have marked an increase in frequency, duration, and severity of wildland fires throughout the world. These wildland fires are a major source of pollutants that are detrimental to human health and visibility.

Mobile scanning lidar is the most appropriate tool for continuously monitoring smoke plumes. However, no practical methodology exists for investigation of smoke-plume dynamics and optical properties with scanning lidar.

This drawback stimulated multi-year studies at the *Fire Sciences Laboratory* (FSL) in Montana, USA. The two-wavelength scanning lidar used in the FSL utilizes two ways for data processing, specified here as Program 1 and Program 2. Program 1 is used to study dynamics of smoke layering and plumes, and to investigate changes of their heights in time and space. For this goal, the lidar data at the 1064 nm wavelength are used. Program 2 focuses on extracting optical parameters of the smoke-polluted atmosphere from lidar signals at the 355 nm wavelength. With Program 2, signal inversion yields vertical profiles for the smoke particulate optical depth, the extinction coefficient profile, and the lidar ratio.

* Paper presented at the "Optoelectronic Techniques for Environmental Monitoring" (OTEM-2009), September 30–October 2, 2009, Bucharest, Romania.

2. ESSENTIALS OF THE INVESTIGATION OF SMOKE-LAYERING AND SMOKE-PLUME DYNAMICS USING PROGRAM 1

The exact boundaries of the smoke plumes and layers are often not well defined, and a large amount of interpretation is generally involved for their identification. In lidar data measured in the vicinities of wildfires, strong diffusion of smoke plumes is commonly observed. This dramatically reduces the intensity and gradients of the backscatter-signal at the smoke plume boundaries, impeding their reliable determination. The use of automated method to determine boundaries between the regions of clear atmosphere and the areas with high level of smoke backscattering is always an issue.

Recently we investigated a new approach, which allows reliable automatic determination of the heights of smoke plumes and layers and their temporal changes using the information obtained for the whole area searched by a scanning lidar [1]. The original signal $P_\Sigma(r)$ recorded by the lidar from the range r is the sum of a backscatter signal $P(r)$ and a constant offset B, created by a daytime background illumination and electrical or digital offset. For the ranges of the complete overlap zone, the signal can be written as,

$$P_\Sigma(r) = \frac{1}{r^2} C\beta_{\pi,tot}(r)[T_{tot}(0,r)]^2 + B \tag{1}$$

where C is a lidar constant, which includes also the transmitted light pulse energy; $\beta_{\pi,tot}(r)$ is the total backscatter coefficient, which is the sum of the molecular and particulate backscatter coefficients, $\beta_{\pi,m}(r)$ and $\beta_{\pi,p}(r)$, respectively; $[T_{tot}(0, r)]^2$ is the total two-way transmission from the lidar to the range r, which is the product of the molecular and particulate components, $[T_m(0, r)]^2$ and $[T_p(0, r)]^2$, respectively. After introducing the new variable defined as $x = r^2$, Eq. (1) can be transformed into the form,

$$Y(x) = P_\Sigma(x)x = C\beta_{\pi,tot}(x)[T_{tot}(0,x)]^2 + Bx\,. \tag{2}$$

Using the local sliding derivative dY/dx over selected ranges, one can determine the corresponding intercept, $Y_0(x)$ with the vertical axis as,

$$Y_0(x) = Y(x) - \frac{\mathrm{d}Y}{\mathrm{d}x}x\,. \tag{3}$$

The calculation of the running numerical derivative dY/dx and the absolute values of corresponding $Y_0(x)$ allows one to identify regions of intense backscatter. The procedure of the identification also includes the normalization of the function $Y_0(x)$ and the determination of the absolute normalized function, $|Y_0^*(r)|$ as a function of range r. The procedure is illustrated in Fig. 1. Here a model profile of the extinction coefficient, $\kappa_t(r)$ is shown as the dotted curve, and the corresponding function, $|Y_0^*(r)|$, as the thick solid curve. One can see that in the smoke plume

area with the increased extinction coefficient, $\kappa_t(r)$ (r = 2200 m - 3900 m), the function $|Y_0^*(r)|$ is much larger than in adjacent clear air regions. Accordingly, the ranges of the near-end sharp increase and the far-end sharp decrease of $|Y_0^*(r)|$ can be considered as boundaries of the smoke plume.

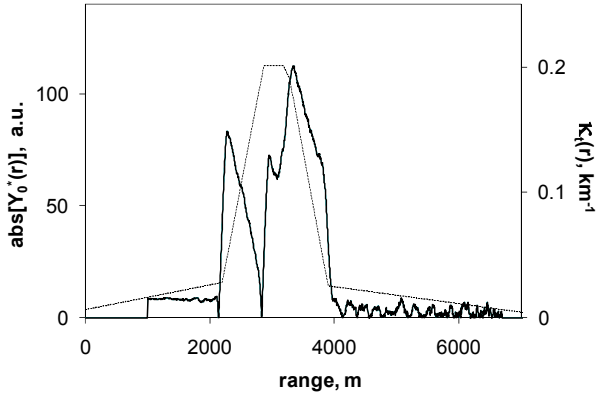

Fig. 1 – Model profile of the smoke-plume extinction coefficient, $\kappa_t(r)$ (the dotted curve), and the corresponding normalized function $|Y_0^*(r)|$ (the thick solid curve).

In Fig. 2, the plot shown is constructed with data from a lidar vertical scan at 1064 nm during the Tripod Complex Fire in the Washington state on August 19, 2006. The lidar scanned vertically over seventy-one slope directions, with elevation angles from 9.5° to 79.5° and angular separation of 1°. This plot is built the same way as the conventional *Range-Height Indicator* (RHI). However, unlike the RHI,

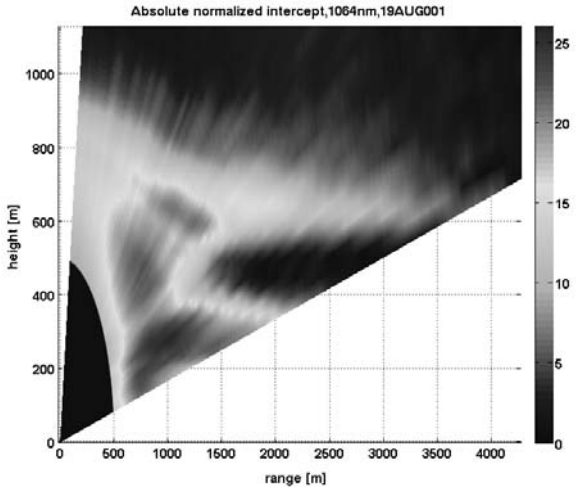

Fig. 2 – Heterogeneity Range-Height Indicator retrieved from the scanning lidar data at 1064 nm during the Tripod Complex Fire in the Washington state on August 19, 2006.

where a colored (or gray) scale shows the relative intensity of the attenuated backscattering, here the scale of the absolute normalized intercept, $|Y_0^*(r)|$, is used. We define the plot in Fig. 2 as the *Heterogeneity Range-Height Indicator* (HRHI). One can see from the figure that the smoke haze is spread up to the heights of 800+ meters. When the dispersed smoke plumes are the subject of interest, such a plot is more informative than the conventional RHI plot.

The above methodology allows creating the so-called atmospheric Heterogeneity Height Indicator (HHI), which shows the heights at which increased smoke-plume backscatter gradients occur and specifies under how many slope directions these gradients were observed. In other words, determination of the smoke boundaries is made through specifying the number of heterogeneity events, $n(h)$, that is, the number of occurrences with increased gradient at each height h.

In Fig 3, the black filled rectangles show data points of the HHI at different heights for the same case as in Fig. 2, and the dashed curve is the corresponding normalized profile of $|Y_0^*(h)|$ for the all seventy-one slope directions. The maximum height where strong atmospheric heterogeneity still exists is h_{max} = 827 m. The HHI makes it possible to identify smoke plume vertical boundaries and their temporal changes using fully automated data processing.

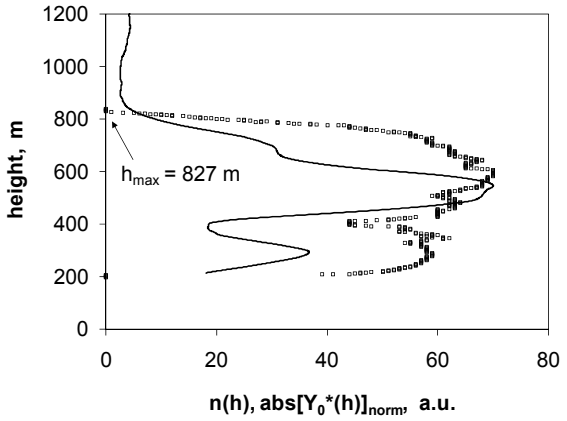

Fig. 3 – Heterogeneity Height Indicator for the case shown in Figure 2 (the empty rectangles) and the corresponding normalized profile of $|Y_0^*(h)|$ (the thick solid curve).

3. ESSENTIALS OF THE INVESTIGATION OF THE STRATIFIED-SMOKE-LAYERING OPTICAL PROPERTIES USING PROGRAM 2

Our consideration of the multiangle mode with Program 2 is restricted by analysis of the Kano-Hamilton multiangle method [2, 3]. This method allows one to avoid an *a priori* selection of the particulate extinction-to-backscatter (lidar) ratio.

The Kano-Hamilton method of the multiangle data processing can be utilized only under favorable conditions. Except horizontal homogeneity, this method requires the condition of a measurable difference for the optical depths under different slope directions. This requirement can be best met if the lidar operates at a short wavelength where the molecular and particulate extinction coefficients are at least comparable. Accordingly, for Program 2, only lidar signals measured at 355 nm are used.

The basic equation of the Kano-Hamilton function is written in the form

$$\ln\left[P_j(h)(h/\sin\varphi_j)^2\right] = A(h) - \frac{2\tau_j(0,h)}{\sin\varphi_j}, \tag{4}$$

where $[P_j(h)[h/\sin\varphi_j]^2$ is the offset-subtracted and square-range-corrected lidar signal at the height h measured at the elevation angle φ_j, and

$$A(h) = \ln\left[C\beta_{\pi,tot}(h)\right], \tag{5}$$

where $\beta_{\pi,tot}(h)$ is the total (molecular and particulate) backscatter coefficient at the height h; $\tau_j(0, h)$ is the total vertical optical depth from the ground level to the height h when measured in the slope direction φ_j within the range from r_{min} to r_{max}. Using the set signals measured along the slope angles φ_1, φ_2, … φ_j,… φ_n, one can define the vertical profiles of $\tau(0, h)$ and $A(h)$ over the heights from h_{min} to h_{max} [4].

3.1. TYPICAL DISTORTIONS IN THE RETRIEVED OPTICAL DEPTH PROFILE

Because of possible inconsistency of the mandatory requirement of the horizontal homogeneity of the searched atmosphere in the Kano-Hamilton method and the lidar signal systematic distortions, the analysis of only random measurement error in multiangle lidar data is not sufficient.

Systematic distortions in the measured lidar signal can be a significant source of measurement uncertainties [5, 6]. The near-end distortions may occur due to inaccuracies in determining the length of the incomplete overlap zone, signal low-frequency noise components, distortions due to the restricted frequency band of the photoreceiver, and receiving optics aberrations. Such distortions generally result in erroneous negative optical-depth values in the near-end range (the dashed curve *aa* in Fig. 4). Accordingly, the minimal acceptable lidar ranges and corresponding heights, r_{min} and h_{min}, should be determined, below which the multiangle measurement data will produce inaccurate measurement results.

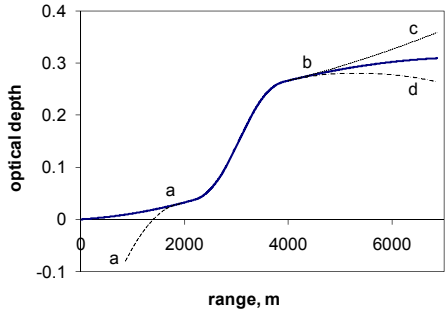

Fig. 4 – True optical depth (the thick solid curve) and possible near-end (curve *aa*) and far-end (curves *bc* and *bd*) distortions caused by the systematic lidar-signal distortions.

Another type of systematic distortions in the retrieved data is found due to the signal offset that remains after subtraction of the signal background component. These distortions are most influential over distant ranges, where the backscatter signal is determined as a small difference of two large quantities. Depending on the sign of the remaining offset, the retrieved optical depth may be either larger or less than the actual value (curves *bc* and *bd* in Fig. 4). It the latter case, the retrieved optical depth can even show an unphysical decrease with the range.

To estimate the uncertainty boundaries in the retrieved profile of the optical depth, $\tau(0, h)$, the analysis of the whole set of vertical profiles derived from each slope-direction scan can be helpful. The set of the vertical profiles $\tau_1(0, h)$, $\tau_2(0, h)$,… $\tau_j(0, h)$,… $\tau_n(0, h)$ can be derived directly from Eq. (4) as

$$\tau_j(0,h) = 0.5 \sin\varphi_j \left\{ A(h) - \ln\left[P_j(h)(h/\sin\varphi_j)^2 \right] \right\}. \quad (6)$$

In Fig. 5, such a set of the individual profiles $\tau_j(0, h)$ measured during the Tripod Fire in Washington state in August 2006 is shown as the grey thin curves; the black

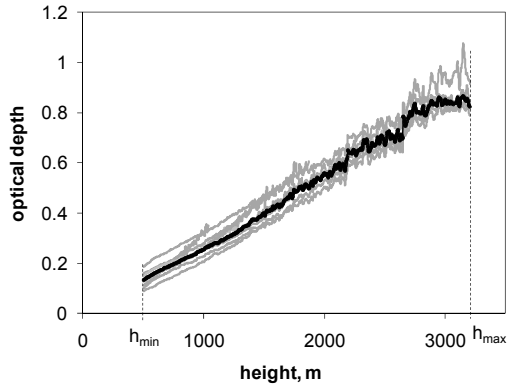

Fig. 5 – Profiles of $\tau(0, h)$ (the thick black curve) and $\tau_j(0, h)$ (the thin gray curves) measured during the Tripod Fire in Washington state.

thick curve is the profile $\tau(0, h)$ obtained from the whole set of the data. Obviously, when estimating uncertainty of the relevant optical parameters extracted from $\tau(0,h)$, the scattering of the individual profiles $\tau_j(0,h)$ should be taken into consideration.

3.2. SPECIFICS OF THE RETRIEVAL OF THE EXTINCTION COEFFICIENT AND THE LIDAR RATIO FROM MULTIANGLE MEASUREMENT DATA

The principal drawback of conventional retrieval techniques used in the multiangle measurement technique is that only the optical depth profile is used for extracting the extinction coefficient. The information concerning particulate loading contained in the backscattering term is generally not used to put additional constraints on the extracted extinction coefficient.

In study [7], an alternative technique is introduced that calculates the extinction coefficient without using numerical differentiation. The underlying principle of this technique assumes that the sharp changes in the lidar ratio are related to sharp changes in the extinction coefficient.

In this new technique, the particulate optical depth $\langle\tau_p(h_n, h_m)\rangle$ over the height interval (h_n, h_m) is calculated using the profile of the integrated backscatter extinction coefficient, $\beta_{\pi,p}(h)$, retrieved with Kano-Hamilton method,

$$\langle\tau_p(h_n, h_m)\rangle = S\int_{h_n}^{h_m}\beta_{\pi,p}(h')dh' . \qquad (7)$$

The basic idea of this technique is to find such a column integrated lidar ratio, S, which provide the best match between the profile, $\langle\tau_p(h_n, h_m)\rangle$ and the profile $\tau_p(h_n, h_m)$, retrieved directly from the Kano-Hamilton solution. After that, the particulate extinction coefficient is determined as the product of S and $\beta_{\pi,p}(h)$. To apply this principle, the uncertainty boundaries in the optical depth profile obtained by the Kano-Hamilton method should be somehow determined, for example, as considered above, in Subsection 3.1.

The variant presented in [7] requires knowledge of lidar constant C. Only in this case, both parameters of interest, the particulate extinction coefficient, $\kappa_p(h)$, and the lidar ratio, S, can be determined. However, our analysis has shown that one of these two parameters, the extinction coefficient, can be determined even if only a very approximate estimate of the constant C is available. To illustrate this observation, some simulation results are presented in Figs. 6–8. In Fig. 6(a) and (b), the model profiles of $C\beta_{\pi,tot}(h)$ and $\tau(0, h)$ used for this simulation are shown.

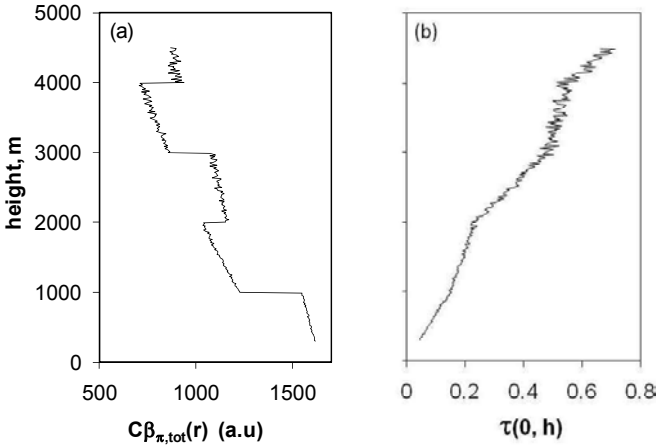

Fig. 6 – Model profiles $C\beta_{\pi,tot}(h)$ and $\tau(0, h)$ [the panels (a) and (b), respectively] used for simulations with different ratios C_{est}/C.

These quasi-random noisy profiles were obtained with an artificial lidar at 355 nm. Fig. 7 shows the profiles of the extinction coefficient, $\kappa_p(h)$ retrieved with method [7], obtained with the assumed uncertainty of the $\tau(0, h)$ equal to ± 0.1 for three different cases. The thick curve is the profile retrieved when the estimated lidar constant, C_{est} is exactly equal to its true value, that is, $C_{est}/C = 1$. The dash-dotted curve is the extinction-coefficient profile obtained when $C_{est}/C = 0.5$ and the gray solid dots represent the profile obtained with the maximum reasonable ratio, $C_{est}/C = 1.3$ (the selection $C_{est}/C > 1.3$ yields unrealistic negative values of the particulate backscatter coefficient). Note that in spite of the inaccuracies in the assumed values

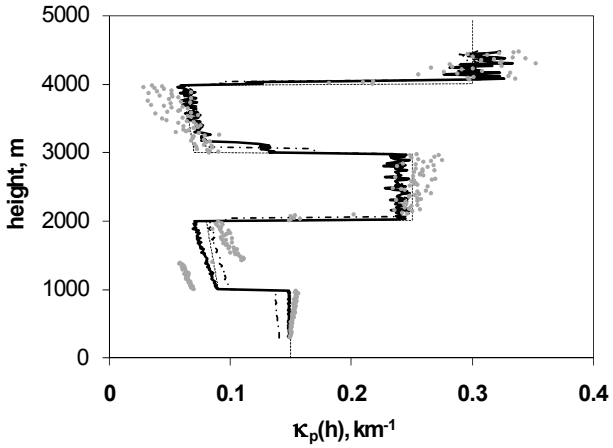

Fig. 7 – Vertical profiles of $\kappa_p(h)$ obtained with different ratios C_{est}/C.

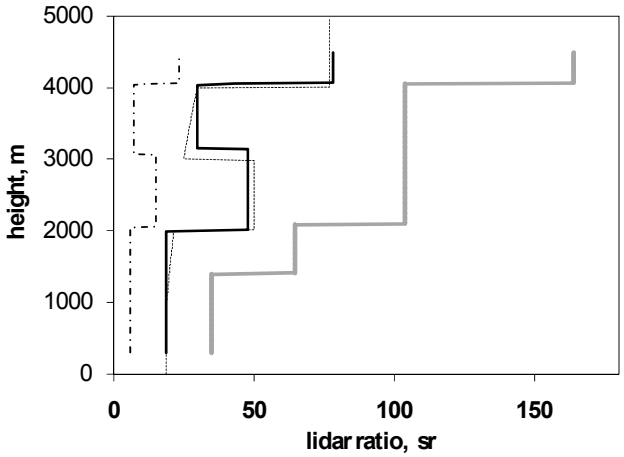

Fig. 8 – Vertical profiles of the column-integrated lidar ratio obtained with different ratios C_{est}/C.

C_{est}, all the retrieved profiles are relatively close to each other and to the "true" (that is, the model) extinction-coefficient profile (the dotted curve) used for the simulation. However, the retrieved lidar ratios (Fig. 8) are significantly different for these cases. The lidar ratio retrieved with $C_{est}/C = 1$ (the thick black curve) is close to the "true" profile (the dotted curve); the selection of $C_{est}/C = 0.5$ yields the lidar ratios that are much less than the real values (the dash-dotted curve), and $C_{est}/C = 1.3$ yields significantly overestimated lidar ratios (the thick gray curve).

4. SUMMARY

Mobile scanning lidar is the best ground-based instrument for monitoring wildfire smoke-plume dynamics and optical properties. It allows continuous monitoring of smoke-polluted atmospheres, providing information about temporal and spatial variation of aerosol properties, plume heights and dynamics, as well as direction and rate of smoke plume movement in near real-time.

In the paper, two different variants for processing scanning lidar data are considered. The first one allows automatic determination of the heights of smoke plumes and layers and their temporal changes using the information obtained for the whole area searched by a scanning lidar. The second variant considers essentials of extracting optical parameters of the smoke polluted atmosphere. It is shown that the extinction coefficient can be derived directly from the backscatter coefficient using the estimate of uncertainty boundaries of the optical depth as a constraint even if the lidar constant is not properly defined.

REFERENCES

1. V. A. Kovalev, A. Petkov, C. Wold, S. Urbanski, and W. M. Hao, *Determination of smoke plume and layer heights using scanning lidar data*, Appl. Opt., **48**, 5287–5294, 2009.
2. M. Kano, *On the determination of backscattered and extinction coefficient of the atmosphere by using laser radar*, Papers Meteorol. and Geophys., **19**, 121– 129, 1968.
3. P. M. Hamilton, *Lidar measurement of backscatter and attenuation of atmospheric aerosol*, Atmos. Environ., **3**, 221–223, 1969.
4. M. Adam, V. A. Kovalev, C. Wold, J. Newton, M. Pahlow, Wei M. Hao, and M. B. Parlange, *Application of the Kano-Hamilton multiangle inversion method in clear atmospheres*, J. Atmosph. & Oceanic Technol., **24**, 2014–2028, 2007.
5. V. A. Kovalev, *Distortions of the extinction coefficient profile caused by systematic errors in lidar data*, Appl. Opt., **43**, 3191–3198, 2004.
6. V. A. Kovalev, W. M. Hao, C. Wold, and M. Adam, *Experimental method for the examination of systematic distortions in lidar data*, Appl. Opt. **46**, 6710–6718, 2007.
7. V. A. Kovalev, W. M. Hao, and C. Wold, *Determination of the particulate extinction-coefficient profile and the column-integrated lidar ratios using the backscatter-coefficient and optical-depth profiles*, Appl. Opt., **46**, 8627–8634, 2007.